

# Fatty Acid Binding Proteins Expressed at the Human Blood–Brain Barrier Bind Drugs in an Isoform-Specific Manner

Gordon S. Lee<sup>1</sup> · Katharina Kappler<sup>1</sup> · Christopher J. H. Porter<sup>1</sup> · Martin J. Scanlon<sup>2</sup> · Joseph A. Nicolazzo<sup>1</sup>

Received: 8 May 2015 / Accepted: 21 July 2015 / Published online: 7 August 2015  
© Springer Science+Business Media New York 2015

## ABSTRACT

**Purpose** To examine the expression of fatty acid binding proteins (FABPs) at the human blood–brain barrier (BBB) and to assess their ability to bind lipophilic drugs.

**Methods** mRNA and protein expression of FABP subtypes in immortalized human brain endothelial (hCMEC/D3) cells were examined by RT-qPCR and Western blot, respectively. FABPs that were found in hCMEC/D3 cells (hFABPs) were recombinantly expressed and purified from *Escherichia coli* C41(DE3) cells. Drug binding to these hFABPs was assessed using a fluorescence assay, which measured the ability of a panel of lipophilic drugs to displace the fluorescent probe compound 1-anilinonaphthalene-8-sulfonic acid (ANS).

**Results** hFABP3, 4 and 5 were expressed in hCMEC/D3 cells at the mRNA and protein level. The competitive ANS displacement assay demonstrated that, in general, glitazones preferentially bound to hFABP5 ( $K_i$ : 1.0–28  $\mu$ M) and fibrates and fenamates preferentially bound to hFABP4 ( $K_i$ : 0.100–17  $\mu$ M). In general, lipophilic drugs appeared to show weaker affinities for hFABP3 relative to hFABP4 and hFABP5. No clear correlation was observed between the molecular structure or physicochemical properties of the drugs and their ability to displace ANS from hFABP3, 4 and 5.

**Conclusions** hFABP3, 4 and 5 are expressed at the human BBB and bind differentially to a diverse range of lipophilic drugs. The unique expression and binding patterns of hFABPs at the BBB may therefore influence drug disposition into the brain.

**KEY WORDS** blood–brain barrier · drug binding · expression profiles · fatty acid binding proteins · fluorescence displacement

## ABBREVIATIONS

ANS	1-anilinonaphthalene-8-sulfonic acid
BBB	Blood–brain barrier
BCECs	Brain capillary endothelial cells
FABP	Fatty acid binding protein
hCMEC/D3	Human immortalized brain endothelial cells

## INTRODUCTION

The blood–brain barrier (BBB) is a critical anatomical structure formed by brain capillary endothelial cells (BCECs) (1). The BBB protects the brain from access of endogenous and exogenous toxins in the systemic circulation through a network of tight junctions, efflux transporter proteins and metabolic enzymes present in BCECs (1). These toxins include harmful metabolites, endogenous and bacterial proteins and exogenous chemicals, including most drugs. As a result, the entry of many drugs into the brain is often restricted by the BBB. This may be beneficial for drugs whose target is in the periphery, but it presents a major barrier for therapeutic agents whose target lies within the central nervous system (CNS) (2). Two major limiting aspects prevent the permeability of many drugs across the BBB: unfavourable physicochemical properties preventing passive diffusion (including high molecular weight and hydrophilicity) and recognition by active efflux transporters (3). In contrast, drugs and endogenous ligands that are able to traverse the BBB exhibit physicochemical properties amenable to permeation by passive diffusion (such as a low molecular weight and moderate lipophilicity), or undergo carrier-mediated transport or receptor mediated endocytosis (4,5).

✉ Joseph A. Nicolazzo  
joseph.nicolazzo@monash.edu

<sup>1</sup> Drug Delivery, Disposition and Dynamics, Monash Institute of Pharmaceutical Sciences, Monash University, 381 Royal Parade Parkville, Victoria 3052, Australia

<sup>2</sup> Medicinal Chemistry, Monash Institute of Pharmaceutical Sciences Monash University, Parkville, Victoria, Australia

Passive transcellular transport of drugs into the CNS is a multifaceted process, however one of the major contributing physicochemical properties driving this process is lipophilicity (4,6). The partitioning of lipophilic drugs from the lumen of the brain capillaries into the mostly lipophilic luminal BCEC membrane is thermodynamically favoured and occurs largely *via* passive diffusion (although some lipophilic drugs are also substrates for membrane transporters) (7,8). In order for lipophilic drugs to permeate the BBB, and to gain entry into the CNS, they must subsequently partition from the luminal membrane of BCECs, diffuse across the aqueous cytosol and traverse the abluminal membrane (7). The dissociation of lipophilic drugs from the luminal membrane into the aqueous cytoplasm of other cells, such as enterocytes, has been reported to be energetically unfavourable (9,10), and a similar scenario may occur at the BBB, with cytosolic transfer of BCECs potentially posing a rate-limiting step in drug transport into the CNS.

Endogenous lipophilic molecules such as fatty acids encounter similar issues in traversing the aqueous cytoplasm of cells. In the case of endogenous lipophilic compounds, numerous *in vitro* and *in vivo* studies have demonstrated that a family of phylogenetically related, low molecular weight proteins - intracellular lipid binding proteins (iLBPs) facilitate ligand access to the aqueous cytoplasm (11,12). One member of the iLBP superfamily, which has been shown to be important in fatty acid trafficking, is the fatty acid binding protein (FABP) family. FABPs are a family of nine small (14–15 kDa) intracellular proteins that are expressed predominantly in tissues that utilize large quantities of fatty acids for energy and lipid biosynthesis (12). In these tissues, FABPs can compose up to 5% of the total soluble cytosolic protein (12). FABPs were originally named after the tissues in which they were first isolated or found to be prominently expressed, however it is now apparent that FABP expression patterns, while specific to different organs, are not exclusive and several FABPs may be co-expressed in a particular organ or cell type. For example, intestinal FABP (FABP2) and liver FABP (FABP1) are both highly expressed in the small intestine (13). FABPs share a common fold in which the binding cavity is formed by 10 antiparallel  $\beta$ -strands folding into a  $\beta$ -barrel, which is capped by two  $\alpha$ -helices (12). The size of the binding cavity of most FABPs is larger than that required to bind a single fatty acid, and several FABPs are able to accommodate other ligands, including some drugs (14–16). For example, rat FABP1 and FABP2 are both able to bind to several classes of lipophilic drugs (17–19). Their role in facilitating drug trafficking has been demonstrated using an artificial intestinal membrane model, where FABP2 was shown to aid in the dissociation and transport of fatty acids and drugs from lipid membranes (9). Furthermore, using an *in vivo* rat model, increasing enterocyte levels of FABP1 and FABP2 by feeding a high fat diet resulted in increased intestinal absorption of ibuprofen,

progesterone and midazolam (drugs that bind rFABP1 and rFABP2), but not propranolol, which does not bind to either rFABP1 or rFABP2 (18). These studies suggest that certain FABPs are able to bind to lipophilic drugs and may contribute to their transport across biological barriers.

It is generally recognized that drugs which cross the BBB are typically lipophilic. Therefore, if FABPs are expressed at the BBB, they may play a role in drug binding and trafficking across the cytoplasm of BCECs. While FABPs have been shown to be expressed in brain parenchymal cells such as neurons (20), there has only been one study reporting the expression of one FABP at the protein level (FABP5) in human brain microvascular endothelial cells (21). This study also demonstrated that FABP5 is involved in the trafficking of palmitic, oleic and linoleic acid across the BBB as genetic silencing of FABP5 resulted in a ~75%, ~46% and ~50% reduction in the transport of these endogenous lipophilic compounds, respectively (21). Whether any of the other 8 FABPs are present at the human BBB, and whether such FABPs have the potential to also bind to lipophilic drugs, remains unclear. The aim of the present study, therefore, was to investigate the gene and protein expression of all FABP isoforms in hCMEC/D3 cells, an immortalized human brain microvascular endothelial cell line (22). A fluorescence displacement assay was then developed and used to assess the binding characteristics of a panel of lipophilic drugs to recombinantly expressed human FABPs that were detected in hCMEC/D3 cells.

## MATERIALS AND METHODS

### Materials

The hCMEC/D3 cell line was obtained from Prof. Pierre-Olivier Couraud (INSERM, France). EBM-2 media and EGM-2 Single Quots Kit were purchased from Lonza (Walkersville, MD). Rat tail collagen type I was purchased from BD Biosciences (Bedford, MA, USA). Penicillin-streptomycin and foetal bovine serum were obtained from Invitrogen (Penrose, Auckland, New Zealand). Cultureware was purchased from Corning Life Sciences (Tewksbury, MA). Dulbecco's Phosphate-buffered saline (D-PBS) was purchased from Life Technologies (Mulgrave, Victoria, Australia). Taqman primers and probes for each hFABP and glyceraldehyde 3-phosphate dehydrogenase (GAPDH) genes were obtained from Applied Biosystems (Foster City, CA). The primary antibody for hFABP3 was purchased from R & D Systems (Minneapolis, MN). Primary antibodies for hFABP4, hFABP5 and  $\beta$ -actin were obtained from Abcam (Cambridge, MA) and the secondary infrared active goat anti-mouse (800 nm) and donkey anti-rabbit (680 nm) antibodies were obtained from Licor (Lincoln, NE). *E. coli* C41(DE3) cells were purchased from Stratagene (Sydney,

New South Wales, Australia) and the expression vectors for hFABP3, hFABP4 and hFABP5 in the pET28a(+) expression system were obtained from DNA2.0 (Menlo Park, CA). 1-anilinonaphthalene-8-sulfonic acid (ANS) was purchased from Sigma-Aldrich (Castle Hill, New South Wales, Australia). Drugs used for binding studies were obtained from Sigma-Aldrich (St Louis, MO), Cayman Chemicals (Ann Arbor, MI) and Tocris Bioscience (Bristol, United Kingdom). Histrap HP and HiTrap Phenyl HP and HiPrep 26/10 Desalting columns were purchased from GE Healthcare Life Sciences (Silverwater, New South Wales, Australia). Milli-Q water was obtained from a Milli-Q water purification system (Millipore, Milford, MA) and all other reagents were of the highest purity commercially available.

### Culturing of hCMEC/D3 Cells

hCMEC/D3 cells were seeded at 50,000 cells/cm<sup>2</sup> and 27,000 cells/cm<sup>2</sup> in 6/24 well plates and T75 flasks, respectively. The cells were grown on cultureware coated with rat-tail collagen type I in the presence of EBM-2 medium supplemented with growth factors from the EGM-2 Single Quots Kit, penicillin-streptomycin and 2.5% *v/v* foetal bovine serum. Cells were cultured at 37°C at 5% CO<sub>2</sub> and saturated humidity and the media was replaced every second day. At 80% confluency, cells were lysed for Western blotting or RNA isolation for subsequent real time reverse transcription polymerase chain reaction (RT-qPCR). The hCMEC/D3 cells used for all experiments ranged between passages 30–36.

### RT-qPCR for mRNA Expression of hFABPs in hCMEC/D3 Cells

At 80% confluency, total RNA from hCMEC/D3 cells was isolated using the Qiagen® RNeasy Mini kit (Hilden, Germany) as per the manufacturer's protocol. The concentration of isolated RNA samples was quantified on a Thermo Scientific® Nanodrop 1000 spectrophotometer (Waltham, MA). The quality of the isolated RNA samples was determined by comparing the absorption ratios between 260/280 nm, with samples exhibiting 260/280 nm ratios of 1.96–2.07 being used for subsequent RT-qPCR.

RT-qPCR was carried out on triplicate samples on a Bio-Rad® C1000 thermocycler (Hercules, CA). Individual RT-qPCR reactions were prepared using the Bio-Rad iScript One-Step® RT-qPCR Kit for Probes (Hercules, CA) as per the manufacturer's protocol. Each reaction mix contained 100 ng of isolated RNA, Taqman primers and probes at a final concentration of 500 nM and 139 nM, respectively, 12.5 µl of RT-qPCR Master mix and nuclease free water to a final volume of 25 µl. The temperature cycle protocol used for reverse transcription and DNA amplification was 10 min

at 50°C, 5 min at 95°C followed by 45 cycles of 10 s at 95°C and 30 s at 60°C. Genes that did not produce amplification profiles before 45 cycles were considered to be below a reasonable level of detection. RNase/DNase free water was used as a negative control. GAPDH was used as a housekeeping gene and the mRNA expression of each of the detected hFABPs was calculated by normalization of their respective C<sub>q</sub> values to that of GAPDH.

### Protein Expression of hFABPs in hCMEC/D3 Cells

Western blot analyses were performed for hFABP3, 4 and 5 from lysate obtained from hCMEC/D3 cells. At 80% confluency, samples were obtained by lysing hCMEC/D3 cells using radio-immunoprecipitation assay (RIPA) buffer (150 mM NaCl, 50 mM Tris base, 1% *v/v* Triton X-100, 0.5% *w/v* sodium deoxycholate, and 0.1% *w/v* sodium dodecyl sulfate (SDS) supplemented with Roche Complete® Protease inhibitor cocktail tablets (Castle Hill, New South Wales, Australia)). In brief, cells were washed with D-PBS and incubated with RIPA buffer at 4°C for 30 min. The samples were then centrifuged at 13614×*g* for 30 min at 4°C and the supernatants were collected and stored at –20°C. The concentration of protein in the supernatants was quantified using a Bio-Rad DC protein assay kit (Hercules, CA), by comparison to standard solutions of bovine serum albumin (BSA) prepared in RIPA buffer.

For protein detection, 15 µg of total protein lysate was mixed with 6X Laemmli buffer (1.2 g SDS, 6 mg bromophenol blue, 4.7 mL glycerol, 1.2 mL 0.5 M Tris HCl) and separated by electrophoresis on a 12% polyacrylamide gel containing a 4% polyacrylamide stacking gel. The Precision Plus Protein Kaleidoscope® ladder from Bio-Rad (Hercules, CA) was used as a molecular weight marker. Following electrophoresis, the separated bands were transferred onto a 0.2 µm nitrocellulose membrane (Bio-Rad, Hercules, CA) *via* a semi dry method using the Bio-Rad® Trans-Blot SD electrophoretic transfer cell (Hercules, CA). After transfer, the membranes were washed 3 times with Tris buffered saline containing 0.1% *v/v* Tween 20 (TBST) followed by a 2 h incubation in Licor® blocking buffer (Lincoln, NE). Blocked membranes were washed 3 times with TBST then incubated overnight at 4°C in Licor® blocking buffer containing primary antibodies for the FABPs and β-actin (housekeeping protein). The primary antibody dilutions for hFABP3, hFABP4, hFABP5 and β-actin were 1:100, 1:500, 1:500 and 1:1000, respectively. After 24 h, the membranes were washed 3 times for 10 min each with TBST, followed by a 2 h incubation with IR active secondary antibodies at 1:30,000 dilution in Licor® blocking buffer. After the incubation period, membranes were washed 3 times for 10 min each with TBST. Imaging of the membranes was performed using the Licor® Odyssey scanner (Lincoln, NE).

### Expression and Purification of Recombinant hFABP3, hFABP4 and hFABP5

Recombinant hFABP3, hFABP4 and hFABP5 were expressed using an *E. coli* C41(DE3)/pET28a host/vector system. C41(DE3) cells were transformed with the different vectors using the heat shock method (23). Transformed cells were cultured in ZYM5052 auto induction media (1% *w/v* tryptone, 0.5% *w/v* yeast extract, 50 mM Na<sub>2</sub>HPO<sub>4</sub>, 50 mM KH<sub>2</sub>PO<sub>4</sub>, 25 mM (NH<sub>4</sub>)<sub>2</sub>SO<sub>4</sub>, 0.5% *w/v* glycerol, 0.05% *w/v* glucose, 0.2% *w/v*  $\alpha$ -lactose and 2 mM MgSO<sub>4</sub>) for 6 h at 37°C followed by 30°C for 24 h at 230 rpm (Multiron orbital shaker, Infors HT, Noble Park North, Victoria, Australia). Cells were harvested by centrifugation (14000 $\times$ *g*, 30 min, 4°C) and were stored at -80°C until protein purification.

The hFABP vectors encoded a hexahistidine tag on the expressed target proteins, allowing the target proteins to be purified by nickel affinity chromatography. Cell pellets were subjected to one freeze-thaw cycle and lysed by sonication in Histrap Buffer A (5 mM imidazole, 250 mM NaCl, 50 mM HEPES, pH 8.0) supplemented with Roche Complete® Protease inhibitor cocktail tablets. Lysates were separated from cell debris by centrifugation at 25000 $\times$ *g* for 30 min at 4°C. The supernatants were syringe-filtered through a 0.22  $\mu$ m nitrocellulose membrane (Pall Life Sciences, Cheltenham, Victoria, Australia) and applied onto a 5 mL Histrap column at 5 mL/min. After loading the sample, the column was washed with Histrap buffer A and proteins were eluted from the column on a gradient of increasing imidazole concentration (5–500 mM) using Histrap buffer B (500 mM imidazole, 250 mM NaCl, 50 mM HEPES, pH 8.0). Fractions containing hFABPs were detected *via* SDS-PAGE, then pooled and ammonium sulphate added to a concentration of 2 M. The resulting solution was applied to a Hitrap Phenyl HP column pre-equilibrated with Buffer C (25 mM Tris, 250 mM NaCl, 2 M (NH<sub>4</sub>)<sub>2</sub>SO<sub>4</sub>, pH 8.0). Bound proteins were eluted on a linear gradient from 2 to 0 M ammonium sulphate over 10 column volumes with Buffer D (25 mM Tris, 250 mM NaCl, pH 8.0). Fractions containing hFABPs were detected *via* SDS-PAGE, pooled and subsequently delipidated by washing twice with a 1:3 *v/v* ratio of butanol:sample by gentle vortexing for 45 s followed by centrifugation at 2880 $\times$ *g* for 2 min at 4°C. The resultant boundary layer containing lipids was removed. To maximize protein stability, delipidated hFABP3 and hFABP5 protein samples were buffer-exchanged into a buffer containing 50 mM HEPES, 100 mM NaCl, 1 mM dithiothreitol (DTT) and 0.5 mM ethylenediaminetetraacetic acid (EDTA), pH 8.0. Delipidated hFABP4 protein samples were buffer-exchanged into a buffer containing 20 mM 2-(N-morpholino)ethanesulfonic acid (MES), 50 mM NaCl, 1 mM DTT, and 0.5 mM EDTA, pH 5.5. Protein samples

were concentrated by ultrafiltration in an Amicon ultra-15 centrifugal filter unit 10 k (Millipore, Kilsyth, Victoria, Australia) prior to storage at 4°C. Protein identity and purity were verified using SDS-PAGE and liquid-chromatography mass spectrometry (LCMS). LCMS was performed on a Luna HPLC C<sub>8</sub> column (Phenomenex, Torrance, CA) with solvent A containing 0.1% *v/v* formic acid in water and solvent B containing 80% *v/v* acetonitrile and 0.1% *v/v* formic acid in water, with all studies conducted on a Shimadzu LCMS-2020 (Canby, OR). Protein concentrations were determined by UV-visible spectrophotometry at 280 nm on a GE Nanovue (Rydalmere, New South Wales, Australia). The extinction coefficients for the hFABPs were calculated from their amino acid compositions using ExPASy (<http://au.expasy.org/tools/protparam.html>). The typical yields of hFABPs following purification and delipidation were 8–10 mg per litre of culture. Initial experiments conducted in the laboratory demonstrated that FABPs with and without the hexahistidine tag displayed no significant differences in binding. Therefore, the hexahistidine tag was not removed from the expressed proteins in order to maximize protein yield. The proteins were stored at 4°C and diluted with their respective buffers to obtain the desired concentrations as required for binding experiments.

### Fluorescence Displacement Assays

The affinity of drugs for different hFABPs was determined by measuring their ability to displace the fluorescent probe molecule ANS. Titrations were carried out in 96-well plates, prepared using a Perkin-Elmer Janus automated liquid handling system using a final volume of between 1030 and 1093  $\mu$ L. It was first necessary to determine the dissociation constant ( $K_d$ ) of each hFABP for ANS. hFABP3, 4 and 5 (1  $\mu$ M) in their respective storage buffers were titrated with ANS (0–16.6  $\mu$ M dissolved in the matching buffers) and binding was monitored by recording the fluorescence of ANS. Steady-state fluorescence was measured on an Envision plate reader (Perkin Elmer, Rowville, Victoria, Australia) by recording emission between 478 and 492 nm using a FITC 485/14 filter following an excitation between 335 and 375 nm using a Umbelliferone 355/40 nm filter. All measurements were performed at 25°C with a minimum of 6 replicates. Since drugs were added from concentrated stocks dissolved in DMSO, the impact of different DMSO concentrations in the buffers on the interaction of ANS and each hFABP was also assessed.

Data modelling operations were performed with GraphPad® Prism version 5.0 software (GraphPad Software, San Diego, CA). The fluorescence signal of ANS was corrected for dilution effects in all experiments. As the  $K_d$  values for ANS binding to the hFABPs were in a similar range to the protein concentration in the

assay, the data were fitted to a one-site ligand depletion hyperbola (Eq. 1)

$$\Delta F = F_{max} \times \frac{([R_T] + [L_T] + K_d) - \sqrt{([R_T] + [L_T] + K_d)^2 - 4[R_T][L_T]}}{2[R_T]} \quad (1)$$

where  $\Delta F$  represents the specific enhancement in the fluorescence intensity of ANS upon its addition to a fixed concentration of hFABP,  $F_{max}$  represents the maximum specific fluorescence enhancement of ANS in the hFABP-ANS complex at saturation,  $K_d$  represents the dissociation constant for ANS binding to hFABP and  $[R_T]$  and  $[L_T]$  represent the total concentration of hFABP and ANS, respectively, used in the experiment.

The binding affinity of a range of lipophilic drugs was determined by monitoring their ability to displace ANS from each hFABP using fluorescence displacement titrations. The molecular structures of the drugs along with their physico-chemical properties calculated using ChemBioDraw 13.0 (CambridgeSoft, Cambridge, MA) are displayed in Table I. Assays were carried out in 96-well plate format. hFABPs (1  $\mu\text{M}$ ) were precomplexed with a saturating concentration of ANS (46.4–60.0  $\mu\text{M}$  for hFABP3, and 24.6–35.3  $\mu\text{M}$  for hFABP4 and hFABP5). Drugs were titrated into the samples from concentrated DMSO stocks. The change in the fluorescence associated with ANS displacement was measured as described above. The DMSO concentration was kept constant at 2.5% *v/v* for all displacement studies. To calculate the  $K_i$  of the ligands for each hFABP, the concentration of compound required to displace 50% of the bound ANS ( $\text{IC}_{50}$ ) was first determined by fitting the fluorescence data to a one-site competition model (Eq. 2)

$$F = F_{min} + (F_{max} - F_{min}) / \left( 1 + 10^{(\text{Log}[L] - \text{Log}[\text{IC}_{50}])} \right) \quad (2)$$

where  $F$  represents the observed fluorescence of ANS at a given concentration of competitive ligand,  $[L]$  represents the concentration of the competing ligand,  $[\text{IC}_{50}]$  is the midpoint of the displacement curve and represents the concentration of competitive ligand required to reduce the initial fluorescence intensity by 50%, and  $F_{min}$  represents the amount of fluorescence produced by ANS when it has been completely displaced by the competitive ligand and is defined as the bottom plateau of the displacement curve. Some drugs had limited solubility at 2.5% *v/v* DMSO which meant that the bottom plateau could not be reached over the concentration range of the displacement titration for certain FABPs. Drugs with limited solubility at 2.5% DMSO have been noted in Table II. In these cases, the data had to be fitted with a bottom plateau that was estimated as the fluorescence of ANS in the absence of hFABPs. To maintain consistency in the interpretation of the data between drugs

that did and did not require this fitting, all curves were fitted with a bottom plateau.

From the calculated  $[\text{IC}_{50}]$ , the  $K_i$  of each drug was determined using the Cheng-Prusoff equation (Eq. 3) (24).

$$K_i = [\text{IC}_{50}] / \left( 1 + \left( \frac{[\text{ANS}]}{K_{d(\text{ANS})}} \right) \right) \quad (3)$$

where  $K_{d(\text{ANS})}$  represents the dissociation constant of ANS for the relevant hFABP and  $[\text{ANS}]$  represents the concentration of ANS precomplexed with the hFABP. All titrations were conducted with 4 replicates.

### Analysis of ANS-FABP Binding by Isothermal Titration Calorimetry

Isothermal titration calorimetry (ITC) was conducted to confirm the binding affinities between ANS and each hFABP determined in the fluorescence assays. ITC experiments were conducted on a MicroCal™ ITC200 system (GE Healthcare, Rydalmere, New South Wales, Australia). In brief, the ITC syringe and cell were washed and the syringe loaded with ANS (500  $\mu\text{M}$ ) in the appropriate hFABP storage buffer and the cell loaded with 50  $\mu\text{M}$  of hFABP. A total of 20 injections were performed with mixing at 1000 rpm and a reference power of 11  $\mu\text{cal/s}$  at 25°C. In the first injection, a 0.2  $\mu\text{L}$  aliquot of the ligand solution was injected into the sample cell over 0.4 s. For all subsequent injections, a 2  $\mu\text{L}$  aliquot of the ligand solution was injected over 4 s. Titrations were conducted with 3 replicates and data modelling operations were performed using the Origin® software (OriginLab, Northampton, MA).

### Statistical Analysis of Data

Statistical analyses were performed using IBM SPSS Statistics 19.0 (IBM Corp, Armonk). A one way analysis of variance (ANOVA) using a Tukey's post-hoc test was used to determine statistical differences between the hCMEC/D3 expression of hFABPs and the binding affinity of the hFABPs to different lipophilic compounds. Independent sample t-tests were used to compare the binding affinities of hFABP3, 4 and 5 to ANS obtained from the ITC and fluorescence assays. All data are presented as mean  $\pm$  S.D unless otherwise stated.

## RESULTS

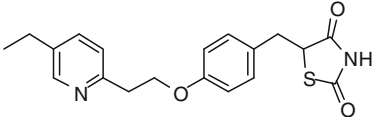
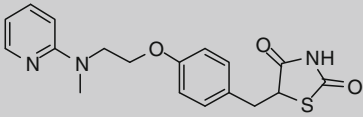
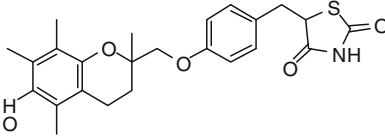
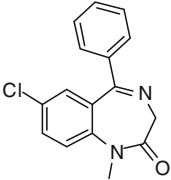
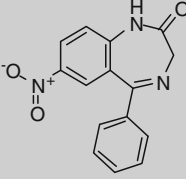
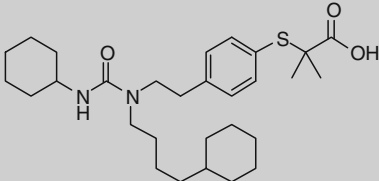
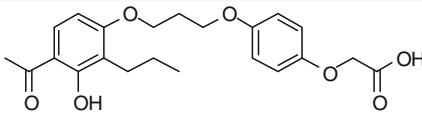
### The Human Blood–brain Barrier Expresses hFABP3, hFABP4 and hFABP5

RNA preparations from hCMEC/D3 cells were analyzed by qRT-PCR for expression of each of the 9 human FABP

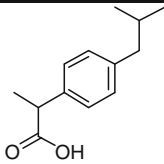
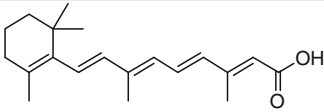
**Table 1** Chemical Structures of the Drugs Investigated in the Binding Studies Against hFABP3, 4 and 5. The Physicochemical Properties of the Compounds were Calculated Using ChemBioDraw Ultra 13.0 (Cambridge Software, MA)

Compound	Molecular structure	Molecular weight (Da)	tPSA ( $\text{\AA}^2$ )	cLogP
<b>Fluorescent probe</b>				
ANS		299.3	66.4	3.7
<b>Fenamates</b>				
Mefenamic acid		241.3	49.3	4.0
Tolfenamic acid		261.7	49.3	4.1
<b>Fibrates</b>				
Bezafibrate		361.8	75.6	3.8
Clofibric acid		214.7	46.5	2.6
Fenofibric acid		318.8	63.6	3.8
Gemfibrozil		250.3	46.5	4.4

Table 1 (continued)

Compound	Molecular structure	Molecular weight (Da)	tPSA ( $\text{\AA}^2$ )	cLogP
<b>Thiazolidinediones</b>				
Pioglitazone		356.4	67.8	3.6
Rosiglitazone		357.4	71.0	3.2
Troglitazone		441.5	84.9	5.1
<b>Benzodiazepines</b>				
Diazepam		284.7	32.7	2.9
Nitrazepam		281.3	93.3	1.6
<b>PPAR agonists</b>				
GW7647		502.8	69.7	6.7
L165041		402.1	102.3	3.1

**Table I** (continued)

Compound	Molecular structure	Molecular weight (Da)	tPSA ( $\text{\AA}^2$ )	cLogP
<b>Propionic acid derivative</b>				
<b>Ibuprofen</b>		206.3	37.3	3.4
<b>Fatty acid</b>				
<b>Retinoic acid</b>		300.4	37.3	4.7

tPSA – Total polar surface area, cLogP – calculated partition coefficient

isoforms (Fig. 1). mRNA for hFABPs3, 4 and 5 (but not other hFABPs) were detected in the hCMEC/D3 cells, expressed at a fraction of 0.62–0.69 that of GAPDH as determined from

analysis of their relative  $C_q$  values. The expression of hFABP3, hFABP4 and hFABP5 proteins in hCMEC/D3 cells was confirmed by Western blots from protein lysate

**Table II** Summary of Inhibition Constants ( $K_i$ ,  $\mu\text{M}$ ) for Various Lipophilic Drugs to hFABP3, 4 and 5 Determined Using the ANS Displacement Assay in the Presence of 2.5% DMSO

Drug Class	Drug	hFABP3	hFABP4	hFABP5
Fenamates	Tolfenamic acid	$1.9 \pm 0.13$	$0.10 \pm 0.040$	$2.9 \pm 0.36$
	Mefenamic acid	$5.8 \pm 0.28$	$1.1 \pm 0.11$	$4.3 \pm 0.65$
Fibrates	Fenofibric acid	$33 \pm 1.3^{a****}$	$24 \pm 2.6^{b****}$	$3.3 \pm 0.33$
	Gemfibrozil <sup>#</sup>	NB	$3.8 \pm 0.19$	$6.1 \pm 1.0$
	Bezafibrate <sup>#</sup>	NB	$12 \pm 1.0$	NB
	Clofibric acid	NB	$17 \pm 0.65$	NB
PPAR agonists	L165041	$14 \pm 0.8^{a*,b*}$	$0.18 \pm 0.03$	$0.21 \pm 0.030$
	GW7647 <sup>#</sup>	$25 \pm 4.21^{a****,b***}$	$7.6 \pm 0.86$	$8.9 \pm 1.1$
Thiazolidinediones	Troglitazone	$11 \pm 1.8$	$16 \pm 2.0^{b***}$	$1.0 \pm 0.080$
	Pioglitazone	$33 \pm 3.0^{b****}$	NB	$11 \pm 1.3$
	Rosiglitazone <sup>#</sup>	NB	NB	$28.8 \pm 5.24$
Propanoic acid derivative	Ibuprofen	$325 \pm 21.8^{a****,b****}$	$2.6 \pm 0.67^{b****}$	$138 \pm 16$
Benzodiazepines	Diazepam <sup>#</sup>	NB	$243 \pm 20^{b****}$	$325 \pm 12.0$
	Nitrazepam	$28 \pm 1.8$	$36 \pm 1.5^{b**}$	$20 \pm 2.5$
Fatty acid	Retinoic acid	$1.3 \pm 0.14$	$1.3 \pm 0.30$	$1.5 \pm 0.35$

Data are presented as mean  $\pm$  SD ( $n = 4$ )

\* $P < 0.05$ , \*\* $P < 0.01$ , \* $P < 0.001$ , \*\*\*\* $P < 0.0001$

NB denotes no binding detected

<sup>#</sup> denotes limited solubility in 2.5% DMSO in experimental buffers

<sup>a</sup> denotes significant difference against hFABP4

<sup>b</sup> denotes significant difference against hFABP5



preparations (Fig. 2). A clear band for hFABP5 and hFABP4 was detected at ~15 kDa, consistent with the molecular weight of FABPs. A band was also present at the correct molecular weight for hFABP3, albeit this was much lighter than that observed for hFABP4 and hFABP5. A positive control of the respective recombinantly-expressed hFABP was loaded onto each gel for reference.

### ANS Binds to hFABP3, hFABP4 and hFABP5 and this is Sensitive to DMSO

Since hFABP3, 4 and 5 were detected in hCMEC/D3 cells at both gene and protein level, these proteins were expressed recombinantly and the ability of drugs to bind to these proteins was assessed using a fluorescence displacement assay. ANS was used as the binding probe as it has been shown to bind to other FABPs and has a low intrinsic fluorescence in aqueous buffer. Titrating ANS into each hFABP (1  $\mu\text{M}$ ) resulted in a concentration dependent, saturable increase in the ANS fluorescence signal (Fig. 3). One-site and two-site binding models were fit to the fluorescence enhancement data and a statistically better fit to a one-site binding hyperbola ( $p < 0.05$ ) was evident. The  $K_d$ 's of ANS binding to hFABP3, hFABP4 and hFABP5 were  $0.63 \pm 0.01 \mu\text{M}$  ( $n=6$ ),  $0.24 \pm 0.04 \mu\text{M}$  ( $n=6$ ) and  $1.32 \pm 0.07 \mu\text{M}$  ( $n=13$ ), respectively (Fig. 4). Since the displacement studies involved addition of the lipophilic drugs from concentrated stocks in DMSO, we next sought to determine whether the  $K_d$  of ANS binding to hFABPs was affected by DMSO. While there was no significant difference in the  $K_d$  values for ANS binding to hFABP4 across the DMSO concentrations tested, the addition of DMSO increased the  $K_d$  of ANS binding to hFABP3 and hFABP5 between 1.5 and 20 fold (Fig. 4). The affinity of ANS binding to each of the three FABPs differs in terms of sensitivity to DMSO as has been previously observed (25). To avoid variation in the binding data obtained in subsequent displacement studies, all ANS-displacement experiments were therefore undertaken in the presence of a constant concentration of DMSO (2.5%) at each titration point. At this

concentration of DMSO, a balance was considered to be achieved; where there was ample DMSO to ensure sufficient solubility of each of the probe drugs (visually assessed by a lack of precipitation) and minimal impact on ANS binding to each hFABP.

To confirm the results of the fluorescence binding studies, ITC was also used to generate  $K_d$  values for ANS binding to each hFABP isoform. A typical isotherm for the binding of ANS to hFABP5 is shown in Fig. 5a, and similar isotherms were observed for ANS binding to hFABP3 and hFABP4. The  $K_d$  values, the enthalpy change, entropy change and the stoichiometry for ANS binding to hFABPs3-5 are shown in Fig. 5b. The stoichiometry ( $N$ ) of binding of ANS to hFABP3-5 was approximately 0.70 suggesting that in each case the hFABPs bound a single molecule of ANS. With all FABPs, binding was accompanied by a favourable change in both the enthalpy ( $\Delta H$ ) and entropy ( $\Delta S$ ), although differences were observed in the relative contribution of the enthalpy and entropy change to the overall change in free energy on binding ( $\Delta G$ ). In the case of hFABP3 and hFABP4, the majority of the change in free energy on binding was derived from the enthalpy change, whereas in the case of hFABP5 the entropy change dominated.

The affinities determined for ANS binding to hFABPs were significantly different when measured by fluorescence studies and ITC (Fig. 6). Comparisons revealed that the  $K_d$  values were within ~25% for hFABP3 and hFABP5 and 50% for hFABP4. Differences between  $K_d$  determined by different biophysical methods are quite common, with 50% not being beyond of what is often observed. For example, the  $K_d$  of the perfluoroalkyl acids, perfluorooctanoic acid and perfluorononanoic acid to FABP1 have been determined to be  $2.36 \pm 0.34 \mu\text{M}$  and  $1.32 \pm 0.20 \mu\text{M}$  by fluorescence displacement titrations and were found to be  $6.49 \mu\text{M}$  and  $3.14 \mu\text{M}$  by ITC (26). Given the higher throughput nature of the fluorescence binding assay it was selected so as to be able to screen a larger number of compounds.

### Drugs Bind to hFABP3, hFABP4 and hFABP5 with Varying Affinities

Displacement of ANS from the hFABPs was measured as the reduction in the fluorescence signal of bound ANS on titration with increasing concentration of the probe lipophilic drugs. The binding isotherms for the lipophilic drugs generally displayed a good fit to a one-site displacement model. Examples of typical binding isotherms (for troglitazone and nitrazepam) are shown in Fig. 7. The inhibition constants ( $K_i$ ) calculated from the binding isotherms of all lipophilic drugs are presented in Table II. All three of the hFABPs were able to bind to a range of the lipophilic drugs examined, although differences in binding affinity were observed across the three hFABP isoforms. The affinity of fatty acid binding to

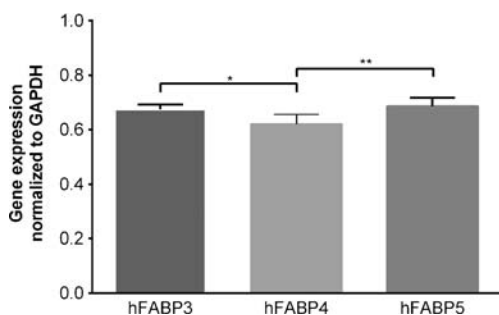


**Fig. 1** Relative gene expression levels of hFABPs in hCMEC/D3 cells normalized to GAPDH. Of the 9 FABPs tested only FABP3, 4 and 5 were detected in hCMEC/D3 cells. Data are presented as mean  $\pm$  SD ( $n=6$ ), \*  $P < 0.05$ , \*\* $P < 0.01$ .

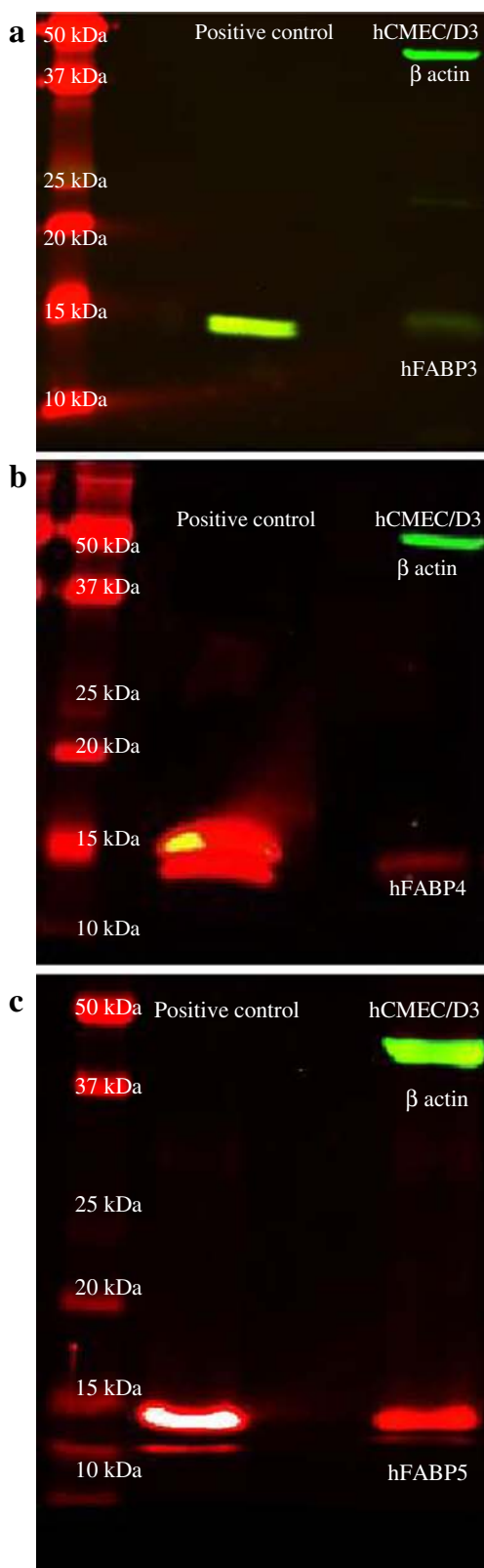


**Fig. 2** Representative Western blots depicting the protein expression of (a) hFABP3, (b) hFABP4, and (c) hFABP5 in hCMEC/D3 cells. A loading of 15  $\mu$ g of total protein was used per lane, with purified recombinant hFABPs serving as positive controls and  $\beta$ -actin serving as a loading control. Bands were observed at positions that were consistent with the expected molecular weight of each protein.

between a membrane and aqueous phase) (27,28). To investigate any relationship between selected physicochemical properties of the lipophilic drugs and binding to the hFABPs, the  $K_i$  was plotted against the  $c\text{Log}P$  and total polar surface area of each lipophilic drug (Fig. 8a-c). No correlation was observed between binding affinity and either  $c\text{Log}P$  or polar surface area for any of the hFABPs tested and each hFABP showed different profiles in these plots. This suggests that the binding is mediated by specific interactions between the drugs and each of the hFABP isoform, rather than non-specific hydrophobic effects.

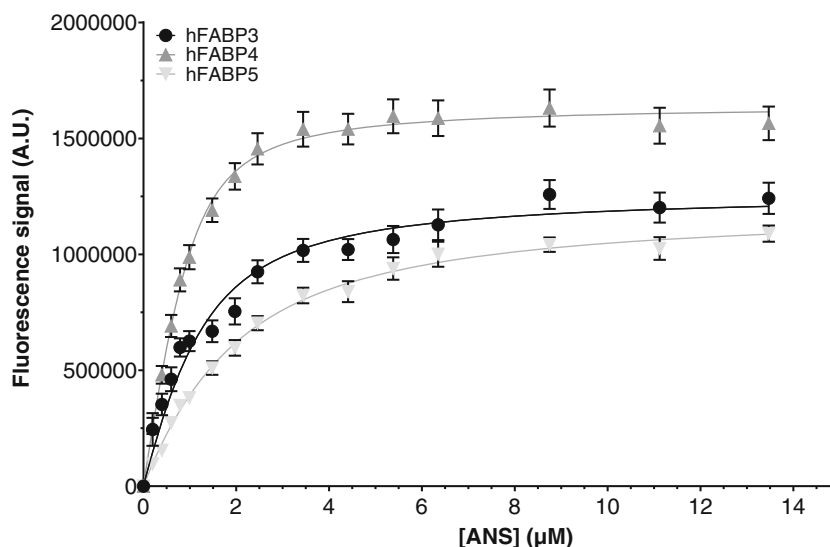
## DISCUSSION

FABPs are a family of iLBP that are important in the trafficking of fatty acids across the aqueous cytosol of different cells, and more recently have been reported to bind to non-fatty acid ligands. For example, FABP1 and FABP2 from both rats and humans can bind to a variety of structurally diverse exogenous ligands and subsequently facilitate their movement across enterocytes (9,18,29). Whether these or other FABPs exhibit a similar function at the BBB is yet to be examined, although it has been demonstrated that FABP5 is important in the trafficking of palmitic acid, oleic acid and linoleic acid across the BBB *in vitro* (21). The purpose of this study was to examine whether/which FABPs are expressed at the human BBB and to assess the binding profile of the identified FABPs to a diverse range of lipophilic drugs with different physicochemical properties and molecular structures.

It has been previously reported that rFABP3 is present in brain microvessels in neonatal rats (30) and that hFABP5 is present in primary human brain endothelial cells (21). In agreement, we report here that hFABP3, hFABP4 and hFABP5 are also expressed at both the gene and protein level in the hCMEC/D3 cell line. This is the first study to demonstrate that hFABP3 and hFABP4 are present in a model of the human BBB and that the expression of these isoforms at the BBB is consistent with their expression in endothelial cells lining the vasculature in other organs (31). Given previous evidence that FABP5 plays a role in the BBB trafficking of palmitic acid, oleic acid and linoleic acid (21), it is possible that hFABP3 and hFABP4 may also be important for the transport of fatty acids across the BBB. Whether FABP5 is involved in the BBB transport of other fatty acids, and whether the isoforms that we have identified in hCMEC/D3 cells affect the CNS disposition of fatty acids *in vivo* requires further

FABPs has been observed previously to show a trend where the affinity is related to the aqueous solubility of the fatty acid (as estimated from the partition coefficient of the fatty acid

**Fig. 3** Binding curve depicting the relationship between the enhancement in ANS fluorescence (absorbance units; A.U.) with increasing concentrations of ANS in the presence of hFABP3, 4 and 5 ( $1 \mu\text{M}$ ). The lines represent the best-fit curves to the one-site ligand depletion model. Data are presented as mean  $\pm$  SD ( $n=6$  for hFABP3-4,  $n=13$  for hFABP5).



study. It is, however, likely that the BBB transport of other fatty acids is modulated by these FABPs given that polyunsaturated fatty acids, a group of fatty acids required in the developing brain, bind to these FABPs with high affinity (20,32,33).

FABPs share a common tertiary structure and bind many of the same fatty acids (12); however, NMR solution structures and crystal structures have demonstrated that different FABPs bind to fatty acids with different conformations. FABP1 can bind to two fatty acids (34); FABP2 binds fatty acids in a bent conformation (35) and FABP3, 4 and 5 bind to fatty acids in a U shape configuration (36–38). This conformation-specific binding appears to be associated with differences in the affinities of FABP binding to specific fatty acids (39). Whether the FABPs identified at the human BBB (*i.e.*, FABP3, 4 and 5) that bind to fatty acids in a similar U shape conformation, preferentially bind to lipophilic drugs with similar characteristics has yet to be thoroughly explored. We therefore used ANS as a

probe and assessed whether hFABP3, 4 and 5 could bind to a panel of drugs using a fluorescence-displacement assay. ANS has been previously used to evaluate drug binding to both rat and human FABP1 and FABP2 (17,19,40). The  $K_d$  values of ANS to these FABPs have been reported to be in the low micromolar range (20,29,41). In the present study, we observe hFABP3, 4 and 5 also bind to ANS within this range. From the fluorescence binding data (Fig. 4), a 2–6 fold difference in the  $K_d$  values for ANS binding to hFABP3, 4 and 5 was evident. This provides an early indication that despite hFABPs3, 4 and 5 binding fatty acids in a similar U-shaped conformation, they appear to exhibit different selectivity towards the same non-fatty acid ligand (*i.e.*, ANS). Furthermore, we observed a difference in the measured thermodynamic signature for the binding of hFABPs3-5 to ANS by ITC (Fig. 5b). Consistent with the binding of fatty acids to FABPs and ANS binding to hFABP2, the binding of ANS to hFABP3, 4 and 5 is accompanied by a favourable change in enthalpy (29,42). However, the entropic contribution towards ANS binding to hFABP3, 4 and 5 is greater than that reported for fatty acid binding to FABPs (42). For FABP3, 4 and 5, the magnitude of the entropy change on binding to ANS was hFABP5 > FABP3 > FABP4. These differences in thermodynamic signatures between the FABPs in this subgroup suggest ANS may bind differently across hFABP3, 4 and 5, as has been suggested by structural studies where ANS was reported to bind to hFABP3 and mFABP4 in opposite orientations (36,42).

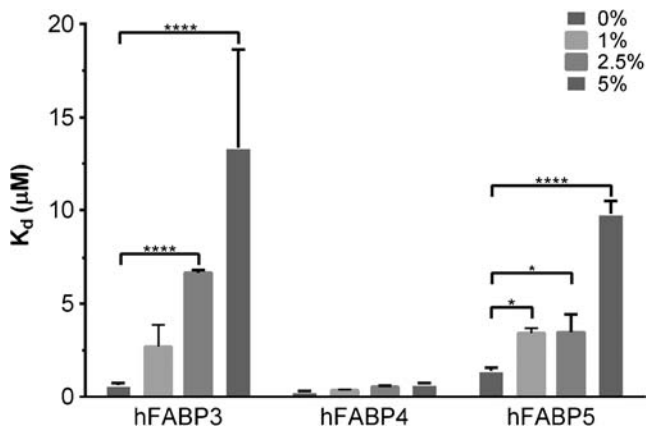


**Fig. 4** The  $K_d$  values for ANS binding to hFABP3, hFABP4 and hFABP5 obtained from the fluorescence titrations in the presence of increasing concentrations of DMSO determined from the best-fit curves. Data are presented as mean  $\pm$  SD, ( $n=4$ –13) \*  $P < 0.05$ , \*\*\*\*  $P < 0.0001$  relative to the absence of DMSO using a one-way ANOVA and post-hoc Tukey test.

Having determined the ability of the fluorescence assay to measure ANS binding, we used this assay to assess whether hFABP3, 4 and 5 were able to bind a range of lipophilic drugs and to investigate potential similarities and differences in the binding selectivity of hFABP3, 4 and 5 for structurally related drugs. Among the fibrates tested, hFABP3 bound only to fenofibric acid, hFABP5 bound to fenofibric acid and

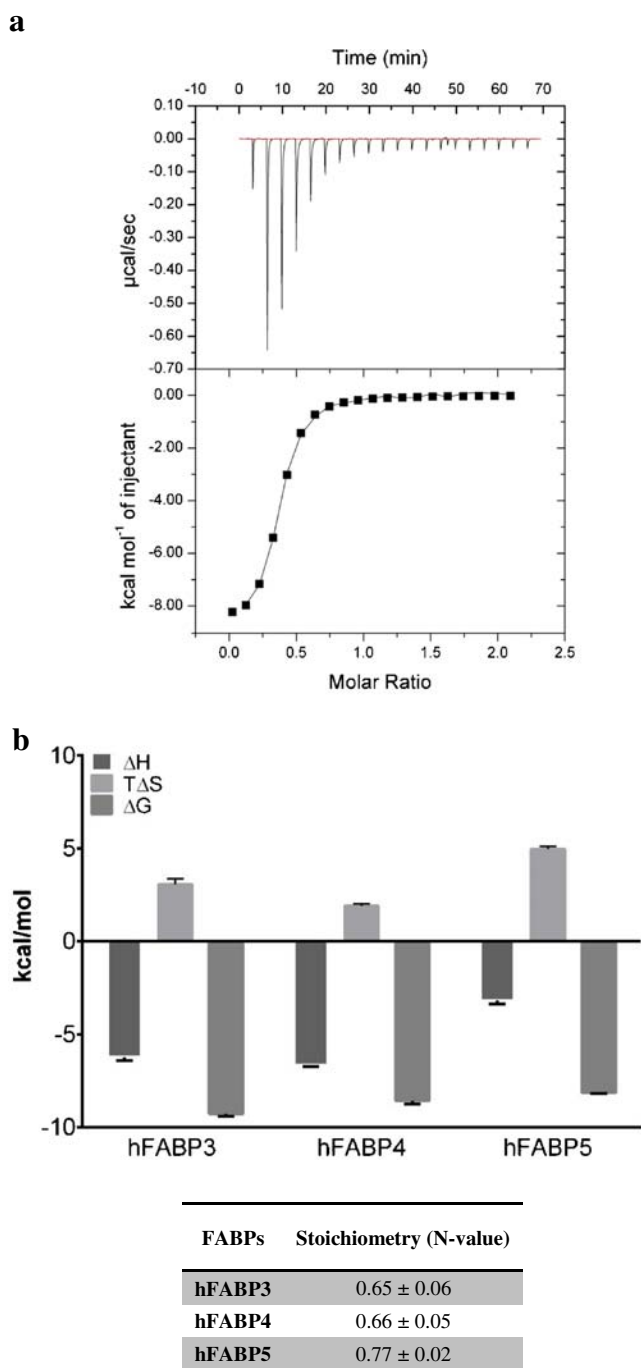


**Fig. 5** (a) A representative ITC binding isotherm for the titration of hFABP5 with ANS. The top panel depicts the heat pulse produced over time for each injection of ANS into the hFABP sample. The bottom panel displays the integrated heat signal with respect to the concentration of ANS and hFABP. (b) Thermodynamic parameters for ANS binding to hFABP3, 4 and 5 determined by ITC. Data are presented as mean ± SD ( $n=3$ ).

gemfibrozil and hFABP4 bound to all the fibrates. In comparison to each other, hFABP4 displayed a 1.6 fold greater affinity for gemfibrozil than hFABP5, whereas hFABP5 displayed a 7.2 fold greater affinity than hFABP4 for fenofibric acid. For the fenamates, while hFABP3, 4 and 5 all bound to both

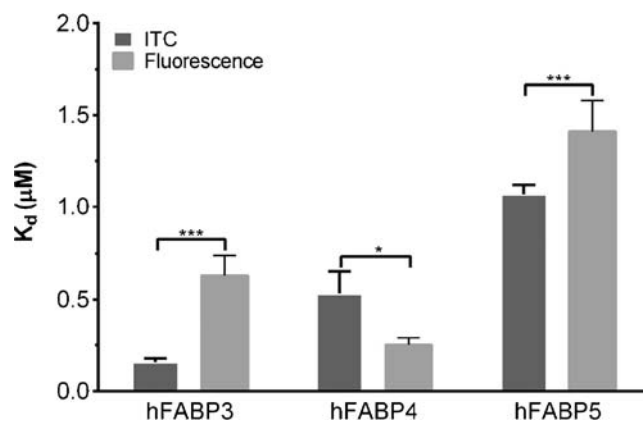


**Fig. 6** Comparisons of the  $K_d$  for ANS binding to hFABP3, 4 and 5 obtained from the fluorescence titrations and ITC. Data are presented as mean ± SD ( $n=3-13$ ) \*  $P < 0.05$ , \*\*\*  $P < 0.001$  using an independent samples t-test.

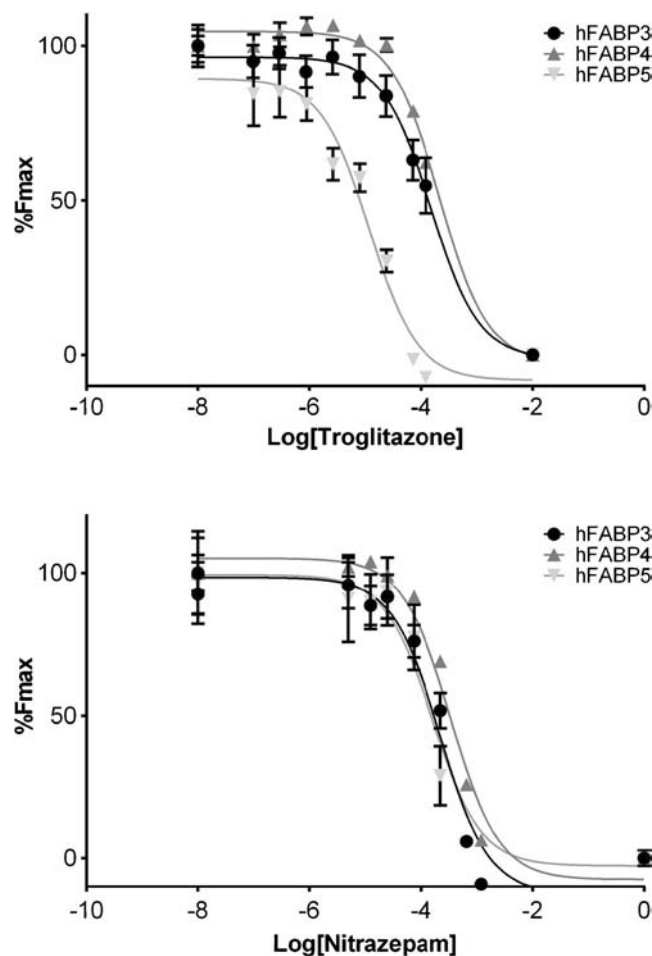


**Fig. 7** Representative displacement curves demonstrating the change in fluorescence of ANS as a result of its displacement by lipophilic drugs from hFABPs. % $F_{max}$  is a measure of the amount of ANS fluorescence detected after its displacement from the hFABPs. Data are presented as mean ± SD ( $n=4$ ).

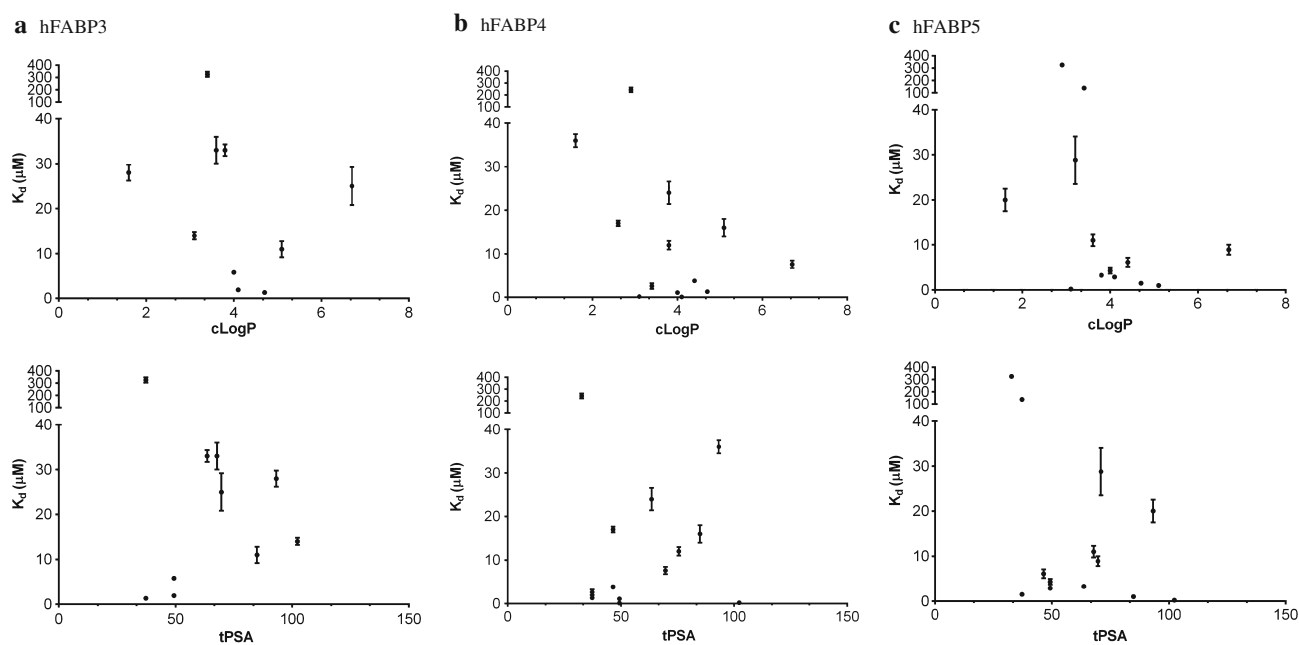


**Fig. 8** The  $K_d$  for various lipophilic drugs to hFABP3, 4 and 5 determined using the ANS displacement assay in the presence of 2.5% DMSO plotted against the drug cLogP and tPSA for (a) hFABP3, (b) hFABP4 and (c) hFABP5. Data are presented as mean  $\pm$  SD ( $n = 4$ ).

mefenamic acid and tolfenamic acid, hFABP4 displayed the highest affinity for both drugs. hFABP4 had a 19 and 29 fold greater affinity for tolfenamic acid and 5.3 and 3.9 fold greater affinity to mefenamic acid relative to hFABP3 and hFABP5, respectively. In general, hFABP4 displayed the highest affinity to the fenamates and fibrates and hFABP5 displayed highest affinity to the glitazones investigated. The binding affinities of drugs to hFABP3, 4 and 5 did not appear to increase with increasing cLogP values, nor was there any apparent relationship between the polar surface area of the lipophilic drugs and their affinities to hFABP3, 4 and 5 (Fig. 8a-c). For example, hFABP5 displayed only a 20 fold lower affinity to rosiglitazone to that of troglitazone, despite the partition coefficient (cLogP) for troglitazone being almost 2 log units higher. The differences in affinity of the same drugs to hFABP3, 4 and 5 suggest that binding to these FABPs is not driven solely by non-specific hydrophobic interactions, but that each hFABP may exhibit specific interactions with lipophilic drugs. It is possible that electrostatic interactions between the drugs and FABPs contribute to the observed binding profiles. Fatty acid binding to FABPs is generally mediated by an electrostatic interaction between the carboxylate of the FA and an arginine residue in the binding cavity of the FABP (17,29). Several of the drugs tested in the current study contain carboxylates, which would most likely be negatively charged under the conditions used for the binding assays. The arginine residues in the cavity of each FABP are also likely to have been positively charged under these assay conditions. However, we have previously shown that the binding of ketorolac to hFABP2 is not mediated by electrostatic interactions, even though ketorolac contains a

carboxylate that is likely to be negatively charged under the conditions used to measure binding (29). Detailed structural characterization of each FABP-drug complex would therefore be necessary to confirm the presence of electrostatic interactions between each FABP and drug.

Whether the FABPs found here to be expressed at the BBB have a significant impact on the CNS disposition of lipophilic compounds remains unknown. The data to date do not provide a clear indication that high affinity to FABPs is associated with a high rate of BBB transport, as compounds such as diazepam, which exhibit high brain uptake *in vivo* (43), do not bind hFABP with high affinity. Further studies are therefore required to assess the functional role of each of the hFABPs in modulating drug transport across the BBB. This might usefully be achieved by silencing each of the hFABPs individually and assessing the impact on drug transport *in vitro* and *in vivo*. It is also possible that drug binding to FABPs may have a more profound impact on drug trafficking to intracellular organelles such as the nucleus, rather than overall drug transport. This has been shown previously for drug binding to FABP1 and FABP2 (44) and FABP4 (44,45). This may govern access to eg. nuclear receptors, and in doing so indirectly alter CNS disposition of their ligands, however, further detailed studies are required to clarify such roles.

## CONCLUSIONS

In the current study, hFABP3, hFABP4 and hFABP5 were found to be expressed at both the mRNA and protein level

in hCMEC/D3 cells. hFABP3, 4 and 5 are capable of binding structurally diverse non-fatty acid lipophilic drug molecules in a manner that is independent of drug class or physicochemical properties. Whether the FABPs detected at the BBB have the potential to modulate the BBB transport of the drugs to which they bind with high affinity is the subject of further investigation.

## ACKNOWLEDGMENTS AND DISCLOSURES

The ANZ Trustees (William Buckland Foundation) and the Australian Research Council (DP120102930) are acknowledged for their financial support of this project.

## REFERENCES

- Abbott NJ, Patabendige AA, Dolman DE, Yusof SR, Begley DJ. Structure and function of the blood-brain barrier. *Neurobiol Dis.* 2010;37:13–25.
- Banks W. Drug transport into the central nervous system: using newer findings about the blood–brain barriers. *Drug Deliv Transl Res.* 2012;2:152–9.
- Loscher W, Potschka H. Role of drug efflux transporters in the brain for drug disposition and treatment of brain diseases. *Prog Neurobiol.* 2005;76:22–76.
- Pajouhesh H, Lenz GR. Medicinal chemical properties of successful central nervous system drugs. *NeuroRx.* 2005;2:541–53.
- Urquhart BL, Kim RB. Blood-brain barrier transporters and response to CNS-active drugs. *Eur J Clin Pharmacol.* 2009;65:1063–70.
- Martinez MN, Amidon GL. A mechanistic approach to understanding the factors affecting drug absorption: a review of fundamentals. *J Pharmacol Clin Toxicol.* 2002;42:620–43.
- Pardridge WM. Drug transport across the blood-brain barrier. *J Cereb Blood Flow Metab.* 2012;32:1959–72.
- Pardridge WM. The blood-brain barrier: bottleneck in brain drug development. *NeuroRx.* 2005;2:3–14.
- Velkov T, Horne J, Laguerre A, Jones E, Scanlon MJ, Porter CJ. Examination of the role of intestinal fatty acid-binding protein in drug absorption using a parallel artificial membrane permeability assay. *Chem Biol.* 2007;14:453–65.
- Velkov T. Thermodynamics of lipophilic drug binding to intestinal fatty acid binding protein and permeation across membranes. *Mol Pharm.* 2009;6:557–70.
- Luxon BA, Milliano MT. Cytoplasmic transport of fatty acids in rat enterocytes: role of binding to fatty acid-binding protein. *Am J Physiol.* 1999;277(2 Pt 1):G361–6.
- Zimmerman AW, Veerkamp JH. New insights into the structure and function of fatty acid-binding proteins. *Cell Mol Life Sci.* 2002;59:1096–116.
- Bass NM, Manning JA. Tissue expression of three structurally different fatty acid binding proteins from rat heart muscle, liver, and intestine. *Biochem Biophys Res Commun.* 1986;137:929–35.
- Hohoff C, Borchers T, Rustow B, Spener F, van Tilbeurgh H. Expression, purification, and crystal structure determination of recombinant human epidermal-type fatty acid binding protein. *Biochemistry.* 1999;38:12229–39.
- He Y, Yang X, Wang H, Estephan R, Francis F, Kodukula S, *et al.* Solution-state molecular structure of apo and oleate-liganded liver fatty acid-binding protein. *Biochemistry.* 2007;46:12543–56.
- Thompson J, Reese-Wagoner A, Banaszak L. Liver fatty acid binding protein: species variation and the accommodation of different ligands. *Biochim Biophys Acta.* 1999;23:1117–30.
- Chuang S, Velkov T, Horne J, Porter CJ, Scanlon MJ. Characterization of the drug binding specificity of rat liver fatty acid binding protein. *J Med Chem.* 2008;51:3755–64.
- Trevaskis NL, Nguyen G, Scanlon MJ, Porter CJ. Fatty acid binding proteins: potential chaperones of cytosolic drug transport in the enterocyte? *Pharm Res.* 2011;28:2176–90.
- Velkov T, Lim ML, Horne J, Simpson JS, Porter CJ, Scanlon MJ. Characterization of lipophilic drug binding to rat intestinal fatty acid binding protein. *Mol Cell Biochem.* 2009;326:87–95.
- Liu JW, Almaguel FG, Bu L, De Leon DD, De Leon M. Expression of E-FABP in PC12 cells increases neurite extension during differentiation: involvement of n-3 and n-6 fatty acids. *J Neurochem.* 2008;106:2015–29.
- Mitchell RW, On NH, Del Bigio MR, Miller DW, Hatch GM. Fatty acid transport protein expression in human brain and potential role in fatty acid transport across human brain microvessel endothelial cells. *J Neurochem.* 2011;117:735–46.
- Weksler BB, Subileau EA, Perriere N, Charneau P, Holloway K, Leveque M, *et al.* Blood-brain barrier-specific properties of a human adult brain endothelial cell line. *FASEB J.* 2005;19:1872–4.
- Froger A, Hall JE. Transformation of plasmid DNA into *E. coli* using the heat shock method. *J Vis Exp.* 2007;6:253.
- Cheng Y, Prusoff WH. Relationship between the inhibition constant (K<sub>1</sub>) and the concentration of inhibitor which causes 50 per cent inhibition (I<sub>50</sub>) of an enzymatic reaction. *Biochem Pharmacol.* 1973;22:3099–108.
- Tjernberg A, Markova N, Griffiths WJ, Hallen D. DMSO-related effects in protein characterization. *J Biomol Screen.* 2006;11:131–7.
- Sheng N, Li J, Liu H, Zhang A, Dai J. Interaction of perfluoroalkyl acids with human liver fatty acid-binding protein. *Arch Toxicol.* 2014;290:13895–906.
- Richieri GV, Ogata RT, Zimmerman AW, Veerkamp JH, Kleinfeld AM. Fatty acid binding proteins from different tissues show distinct patterns of fatty acid interactions. *Biochemistry.* 2000;39:7197–204.
- Kleinfeld AM, Chu P, Romero C. Transport of long-chain native fatty acids across lipid bilayer membranes indicates that transbilayer flip-flop is rate limiting. *Biochemistry.* 1997;36:14146–58.
- Patil R, Laguerre A, Wielens J, Headey SJ, Williams ML, Hughes ML, *et al.* Characterization of two distinct modes of drug binding to human intestinal fatty acid binding protein. *ACS Chem Biol.* 2014;9:2526–34.
- Pelerin H, Jouin M, Lallemand MS, Alessandri JM, Cunnane SC, Langelier B, *et al.* Gene expression of fatty acid transport and binding proteins in the blood-brain barrier and the cerebral cortex of the rat: differences across development and with different DHA brain status. *Prostaglandins Leukot Essent Fat Acids.* 2014;91:213–20.
- Hagberg C, Mehlem A, Falkevall A, Muhl L, Eriksson U. Endothelial fatty acid transport: role of vascular endothelial growth factor B. *Physiology.* 2013;28:125–34.
- Bachmeier C, Mullan M, Paris D. Characterization and use of human brain microvascular endothelial cells to examine beta-amyloid exchange in the blood-brain barrier. *Cytotechnology.* 2010;62:519–29.
- Balendiran GK, Schmutgen F, Scapin G, Borchers T, Xhong N, Lim K, *et al.* Crystal structure and thermodynamic analysis of human brain fatty acid-binding protein. *J Biol Chem.* 2000;275:27045–54.

34. Thompson J, Winter N, Terwey D, Bratt J, Banaszak L. The crystal structure of the liver fatty acid-binding protein. A complex with two bound oleates. *J Biol Chem.* 1997;272:7140–50.
35. Scapin G, Young AM, Kromminga A, Veerkamp J, Gordon J, Sacchettini J. High resolution X-ray studies of mammalian intestinal and muscle fatty acid-binding proteins provide an opportunity for defining the chemical nature of fatty acid: protein interactions. *Mol Cell Biochem.* 1993;123:3–13.
36. Hirose M, Sugiyama S, Ishida H, Niiyama M, Matsuoka D, Hara T, *et al.* Structure of the human-heart fatty-acid-binding protein 3 in complex with the fluorescent probe 1-ranilidonaphthalene-8-sulphonic acid. *J Synchrotron Radiat.* 2013;20:923–8.
37. Gillilan RE, Ayers SD, Noy N. Structural basis for activation of fatty acid-binding protein 4. *J Mol Biol.* 2007;372:1246–60.
38. Gutierrez-Gonzalez LH, Ludwig C, Hohoff C, Rademacher M, Hanhoff T, Ruterjans H, *et al.* Solution structure and backbone dynamics of human epidermal-type fatty acid-binding protein (E-FABP). *Biochem J.* 2002;364:725–37.
39. Zimmerman AW, Rademacher M, Ruterjans H, Lucke C, Veerkamp JH. Functional and conformational characterization of new mutants of heart fatty acid-binding protein. *Biochem J.* 1999;344(Pt 2):495–501.
40. Velkov T. Interactions between human liver fatty acid binding protein and peroxisome proliferator activated receptor selective drugs. *PPAR Res.* 2013; 938401.
41. Kane CD, Bernlohr DA. A simple assay for intracellular lipid-binding proteins using displacement of 1-anilidonaphthalene 8-sulphonic acid. *Anal Biochem.* 1996;233:197–204.
42. Richieri GV, Ogata RT, Kleinfeld AM. Fatty acid interactions with native and mutant fatty acid binding proteins. *Mol Cell Biochem.* 1999;192:77–85.
43. Bergstrom CA, Charman SA, Nicolazzo JA. Computational prediction of CNS drug exposure based on a novel in vivo dataset. *Pharm Res.* 2012;29:3131–42.
44. Hughes ML, Liu B, Halls ML, Wagstaff KM, Patil R, Velkov T, *et al.* Fatty acid binding proteins 1 and 2 differentially modulate the activation of peroxisome proliferator-activated receptor alpha in a ligand-selective manner. *J Biol Chem.* 2015.[In Press]
45. Tan NS, Shaw NS, Vinckenbosch N, Liu P, Yasmin R, Desvergne B, *et al.* Selective cooperation between fatty acid binding proteins and peroxisome proliferator-activated receptors in regulating transcription. *Mol Cell Biol.* 2002;22(14):5114–27.